RECENT ADVANCES IN CALIFORNIA CURRENT MODELING: DECADAL AND INTERANNUAL THERMOCLINE VARIATIONS

ARTHUR J. MILLER
Climate Research Division
Scripps Institution of Oceanography
La Jolla, California 92093-0224

ABSTRACT

Some recent advances in large-scale modeling of the California Current and its interaction with basin-scale circulation and forcing are summarized. The discussion concentrates on a decadal-scale change and interannual-scale variations identified in the thermocline off the California Coast. The western-intensified decadal-scale change is part of a basinwide change in the North Pacific thermocline from the early 1970s to the early 1980s, which has been observed and modeled. The decadal change is driven by a basin-scale change in wind stress curl (Ekman pumping) and is associated with a deepening of the thermocline off California but no significant change in the strength of the California Current. Interannual variations of the thermocline off the California Coast, which tend to be associated with ENSO, have also been observed and modeled. High-resolution models often exhibit a coastal-trapped Kelvin-like wave arriving from the equatorial zone, but even a coarse-resolution model can capture aspects of the midlatitude wind-forced thermocline signals that propagate westward on ENSO time scales.

INTRODUCTION

Models of the California Current System (CCS) have been in development as long as numerical simulation has been a part of oceanography. Many fundamental issues have been central to the various strategies for formulating models. Among these issues are: why there is an eastern boundary current in the first place (e.g., Philander and Yoon 1982; McCreary et al. 1992); what controls interannual variations of the current (e.g., Pares-Sierra and O'Brien 1989); why such a strong eddy field exists in a relatively weak mean current (e.g., Batteen et al. 1989; Auad et al. 1991; Hurlburt et al. 1992); whether the eddy field can be numerically forecast (e.g., Robinson et al. 1984; Rienecker et al. 1987); what controls the occurrence of cold filaments (e.g., Haidvogel et al. 1991; Allen et al. 1991); and how cold filaments influence biological productivity (e.g., Moisan and Hofmann 1996a, b; Moisan et al., in press).

I can address here only a small subset of the interesting issues and important advances that have occurred in modeling the CCS. Specifically, I discuss in the next two sections a decadal-scale change in the thermocline off the California coast, which has been recently modeled in a coarse-resolution model, and the physics that control observed and modeled interannual variations in the CCS thermocline and velocity field. I concentrate on model results that may be directly compared with observations for validation.

A DECADAL-SCALE CHANGE IN THE NORTH PACIFIC THERMOCLINE

Decadal-scale changes have been observed in numerous physical, chemical, and biological variables in the North Pacific (e.g., Douglas et al. 1982; Ebbesmeyer et al. 1991; Roemmich and McGowan 1995). One especially interesting change occurred in the mid-1970s (e.g., Trenberth 1990; Graham 1994; Trenberth and Hurrell 1994) for which, in previous work (Miller et al. 1994a, b), we have attempted to explain the oceanic physics involved in switching the ocean from a warm central (cool eastern) North Pacific state to an oppositely signed regime after the winter of 1976–77.

A recent observational and modeling study identified a basin-scale change in the oceanic thermocline in the North Pacific.[1] A data set of upper-ocean (to 400-m depth) XBT observations from the period 1970–88 (for details, see White 1995) was compared with the response of an ocean general-circulation model forced by observed fluxes and winds over the same period. The model is a primitive equation formulation constructed with eight isopycnic layers (of variable temperature, salinity, and thickness), which are fully coupled to a bulk surface mixed-layer model. The run is forced by observed monthly mean anomalies of wind stress, heat flux, and turbulent kinetic energy input to the mixed layer. Although the resolution is rather coarse—nominally four degrees but with enhanced resolution near the equator and boundaries (figure 1)—the results are unique in that we are unaware of any other North Pacific Ocean simulation which is forced over such a long period (1970–88) with both wind-stress and surface-flux forcing.

The dominant signal common to both model and observation has decadal scale and is illustrated in figure 2, which shows differences in the upper-ocean tempera-

---

[1]Miller, A. J., D. R. Cayan, and W. B. White. A decadal change in the North Pacific thermocline and gyre-scale circulation. MS submitted to J. Clim.

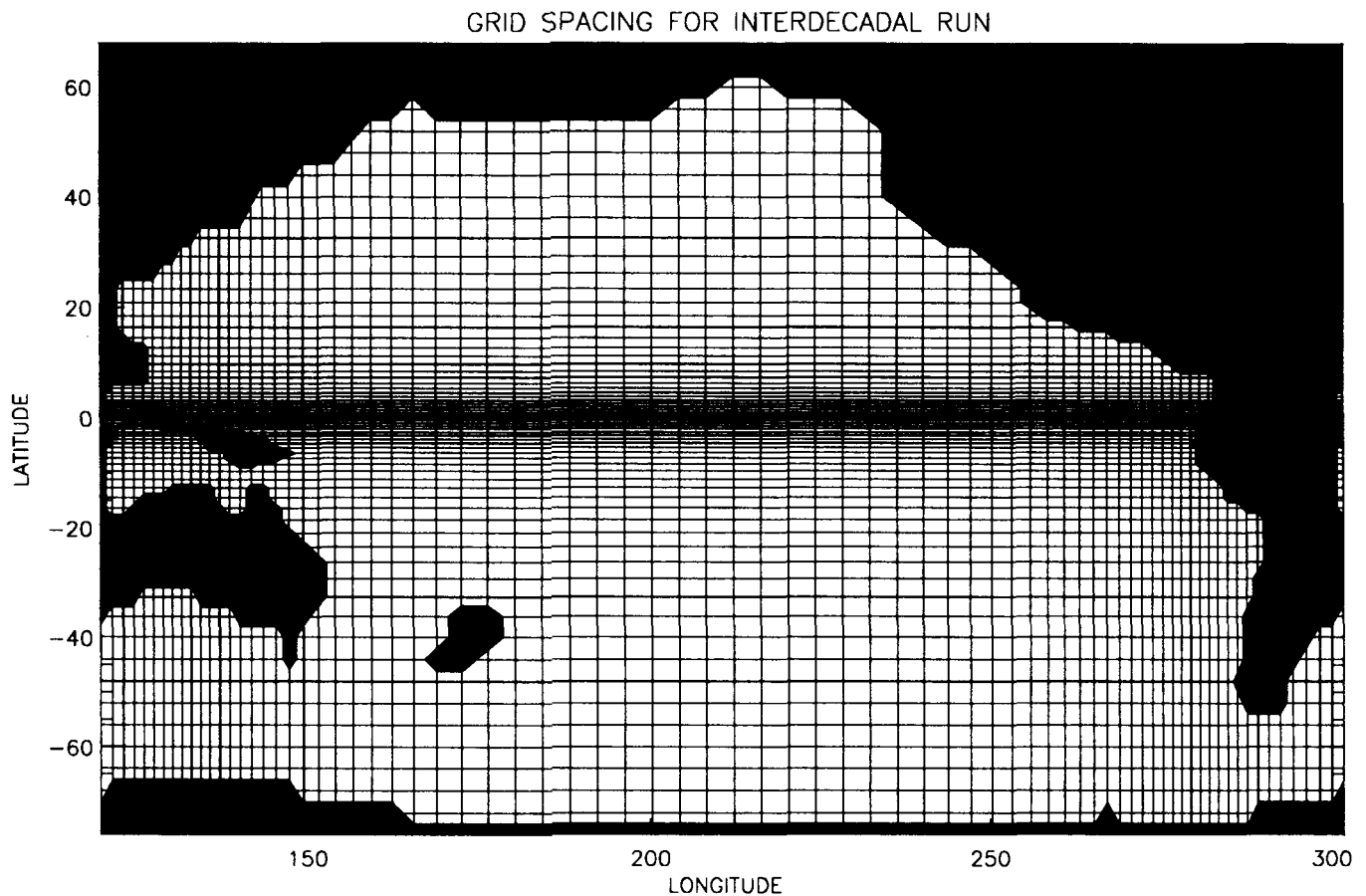## GRID SPACING FOR INTERDECADAL RUN

Figure 1.   Geometry and grid of the isopycnic coordinate model developed by Oberhuber (1993) and applied by Miller et al. (1994a, b; MSS; see footnotes 1 and 5) for interannual through interdecadal studies of the Pacific Ocean, as discussed in the text.

ture field of the North Pacific from the early 1970s to the early 1980s. In the surface mixed layer, one sees the well-known structure of cooling in the central Pacific and warming of the eastern Pacific. This structure is commensurate with the large-scale structure of the atmospheric variables (heat fluxes and wind stresses) which drive the variability (Cayan 1992; Miller et al. 1994a, b). The time series of sea-surface temperature (SST) variability in a region off western North America (130°W–coast, 24°N–44°N) reveals a good correspondence between model and observations and also the step-like character of the SST change during the winter of 1976–77 (figure 2). Miller et al. (1994a, b) showed that heat fluxes and horizontal advection both contributed to the shift in SST which occurred off western North America during the 1976–77 winter, and that surface heat fluxes were the primary maintenance mechanism for preserving the regimes there before and after the shift.

Looking beneath the mixed layer at 200 m and 400 m (figure 2), where little or no direct contact with the atmosphere occurs, one sees a progression into regions where ocean dynamics are expected to dominate the re-

sponse. Indeed, the thermal structures at 400 m bear a western-intensified structure reminiscent of gyre-scale circulation theory. Because the mean thermocline is shallower off the coast of California than it is in the middle of the Pacific, I plot temperature anomalies at 120 m (figure 2, bottom) to show that the thermocline deepened from the early 1970s to the early 1980s at the same time that it was raised (cooler 400-m temperature) in the northwestern Pacific. The time series of 120-m temperature variations also shows that the model captures both the deepening of the thermocline as well as interannual variations (to be discussed in the next section). Both data and the model reveal that a more gradual change in temperature occurs at depth (cf. Deser et al. 1996) in comparison to the steplike change in the surface layer.

Difference maps like figure 2 are useful for understanding gross features of the response, but they fail to give a clear picture of the coherency of variations over large spatial and long temporal scales. Empirical orthogonal function (EOF) analysis is useful for just such a purpose. In order to better isolate stationary features from
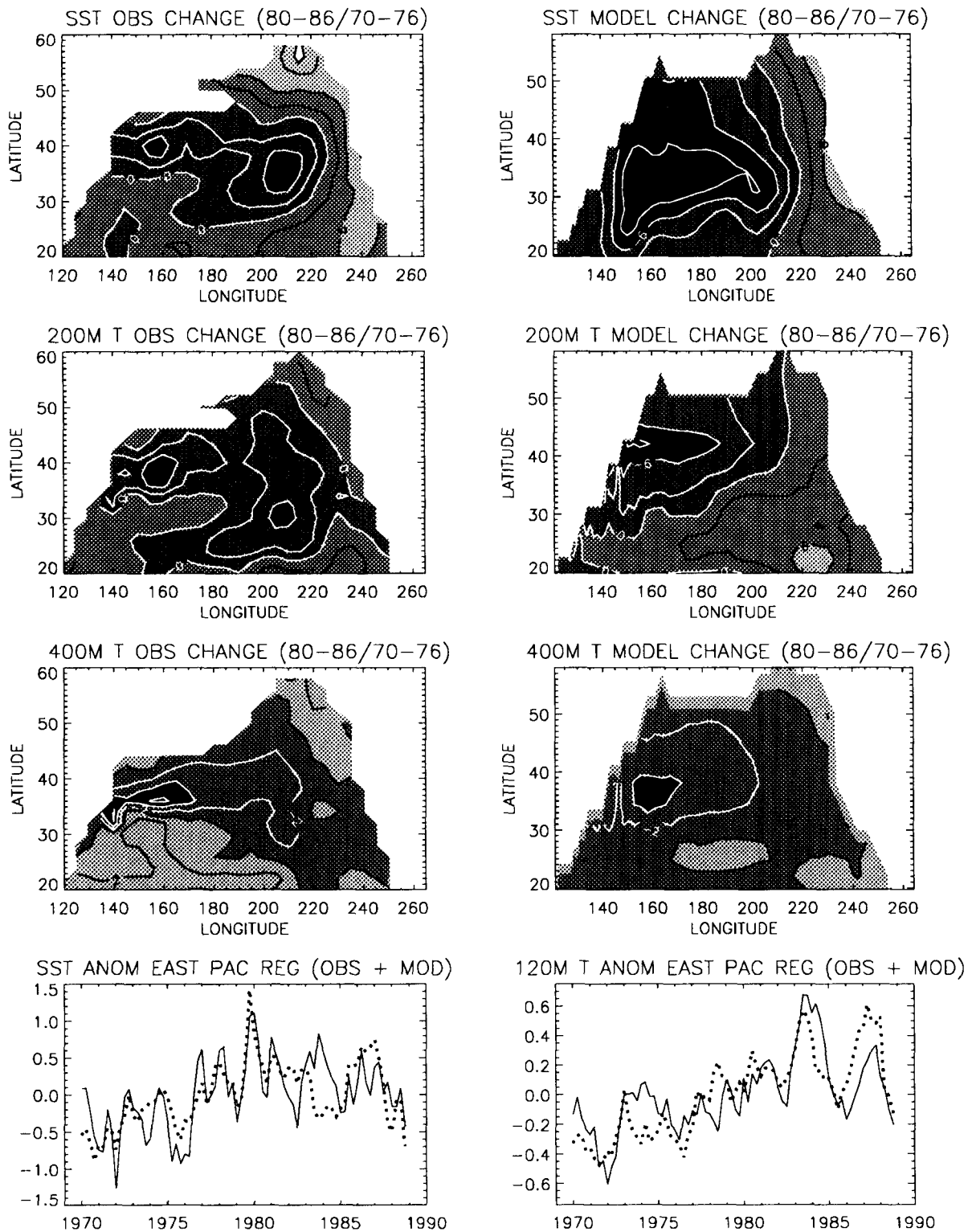
Figure 2. Difference maps of the 7-year periods 1980–86 relative to 1970–76 for (*top*) sea-surface, (*middle*) 200-m, and (*lower*) 400-m temperature for (*left*) observations and (*right*) model. For SST and 200-m temperature, contour intervals are 0.3°C (zero and negative contours white); for 400-m temperature, contour intervals are 0.2°C (zero and positive contours black), with darker shading negative and lighter shading positive. Time series (*bottom*) of observed (*solid line*) and modeled (*dotted line*) temperature at surface (*left*) and 120 m (*right*), averaged over the eastern Pacific region 130°W–coast, 24°N–44°N.

propagating ones, Miller et al.[2] used extended EOF (EEOF) analysis of observed 400-m temperature, model 400-m temperature, model 400-m velocity, and wind stress curl forcing to isolate the decadal-scale signal. Only the region of the North Pacific east of 155°E and north of 20°N was considered in order to avoid including the poorly resolved (in both the model and XBT data set) Kuroshio region and the ENSO-dominated low latitudes.

Figure 3 shows a synopsis of the EEOF view of the basin-scale decadal temperature change in observations and in the model.[3] Since this mode is nearly stationary, we plotted the average of the 13 lags together rather than showing the lags for individual phases. The top two maps show the first combined EEOF of observations and model 400-m temperature, with the time series (scaled amplitude) shown as the thin line in the bottom plot. (The two temperature fields are normalized by 0.25°C and 0.13°C, respectively, because model variability is weaker than observed.) The observed pattern is essentially the same as that of the first EEOF of observations alone (not shown), and the combined EEOF time series has time variation very similar to the EEOF of observations alone. Both the model and observations reveal a cooling of the basin-scale 400-m temperature (a shoaling of the thermocline) from the early 1970s to the early 1980s (as seen in the time coefficient), which is western intensified as expected from inspection of figure 2.

Since this signal explains 29% of the combined variance, it represents a significant deviation of the basin-scale thermocline structure and can be expected to be associated with gyre-scale changes in upper-ocean circulation. Indeed, the combined EEOF of model 400-m temperature and model 400-m velocity (second panel of figure 3 and dotted time series at bottom) reveals that the decadal signal is nearly geostrophically balanced over this 10-year transition time scale. The flow field reveals a 10% increase in the strength of the Kuroshio extension and the subpolar gyre return flow (cf. Sekine 1991; Trenberth and Hurrell 1994). A stronger than normal northward flow into the central Gulf of Alaska (cf. Tabata 1991; Lagerloef 1995) is also seen during the early 1980s in the model diagnosis.

It is interesting to note that little change in the California Current System is associated with this decadal signal, even though the thermocline (figures 2 and 3) did deepen off the west coast of America. A basin-scale change in wind stress curl is the driving mechanism for the thermocline change. Combined extended EEOFs of wind stress curl and north-south transport (integrated from 0 m to 1,500 m) yield an EEOF mode (third panel

of figure 3 and dashed time series at bottom) that corresponds to the decadal change in temperature and velocity (panels 1 and 2). Figure 3 indicates that in the eastern basin the flow field is nearly in a local Sverdrup balance (to within a factor of two), and supports the notion that the wind stress is the forcing function of the decadal thermocline change. Note, however, that Meyers et al. (in press) suggest that the thermocline change in the California coastal region may be influenced by waves arriving along the eastern boundary from the tropics.

ENSO-SCALE THERMOCLINE VARIATIONS

The time series in figures 2 and 3 reveal interannual variations in the thermocline associated with time scales of El Niño and the Southern Oscillation (ENSO). Understanding what forces these fluctuations has been a lively subject, and models have successfully reproduced many aspects of the CCS response.

The central question is whether the variations are primarily driven by local forcing such as winds or whether the changes arrive from the equatorial region via coastally trapped Kelvin-like waves. Pares-Sierra and O'Brien (1989) addressed the question directly by using a shallow-water model which resolves the baroclinic deformation radius along eastern Pacific boundary. They compared the results of three simulations with observed sea level. One run was forced by midlatitude winds, a second by oceanic waves propagating north along the eastern boundary from the tropics, and a third by the two effects combined. Pares-Sierra and O'Brien's results demonstrated that local sea level along western North America has an interannual component which arrives through the ocean from the tropics.

Further studies in that modeling framework included those of Johnson and O'Brien (1990)—who showed that an additional component of interannual response is driven by the atmosphere at higher latitudes—and of Shriver et al. (1991)—who identified observed thermocline anomalies along 40°N that corresponded to model baroclinic waves radiated from the coastally trapped signal of equatorial origin. Jacobs et al. (1994, 1996[4]) found that model baroclinic waves radiating from the coastally trapped Kelvin-like waves of the 1982–83 ENSO were able to propagate intact across the Pacific and arrive near the Kuroshio region some ten years later. Ramp et al. (1996) studied a primitive equation model (Smith et al. 1992) forced by ECMWF winds from 1985 to 1994 and found competing effects off California of local winds driving the response, as well as coastal oceanic waves (which may have been scattered into higher vertical

---

[2]See footnote 1 on p. 69.

[3]See footnote 1 on p. 69.

[4]Jacobs, G. A., H. E. Hurlburt, and J. L. Mitchell. Decadal variations in ocean circulation, part I: Rossby waves in the Pacific. MS submitted to J. Geophys. Res.

EEOF1 400M T-OBS 13LAGAV

EEOF1 400M T-MODEL 13LAGAV

EEOF-1 400M UV-MODEL, 13LAGAV

EEOF-1 400M T-MODEL 13LAGAV

EEOF-3 RHO-H-VBAR 4LAGAV
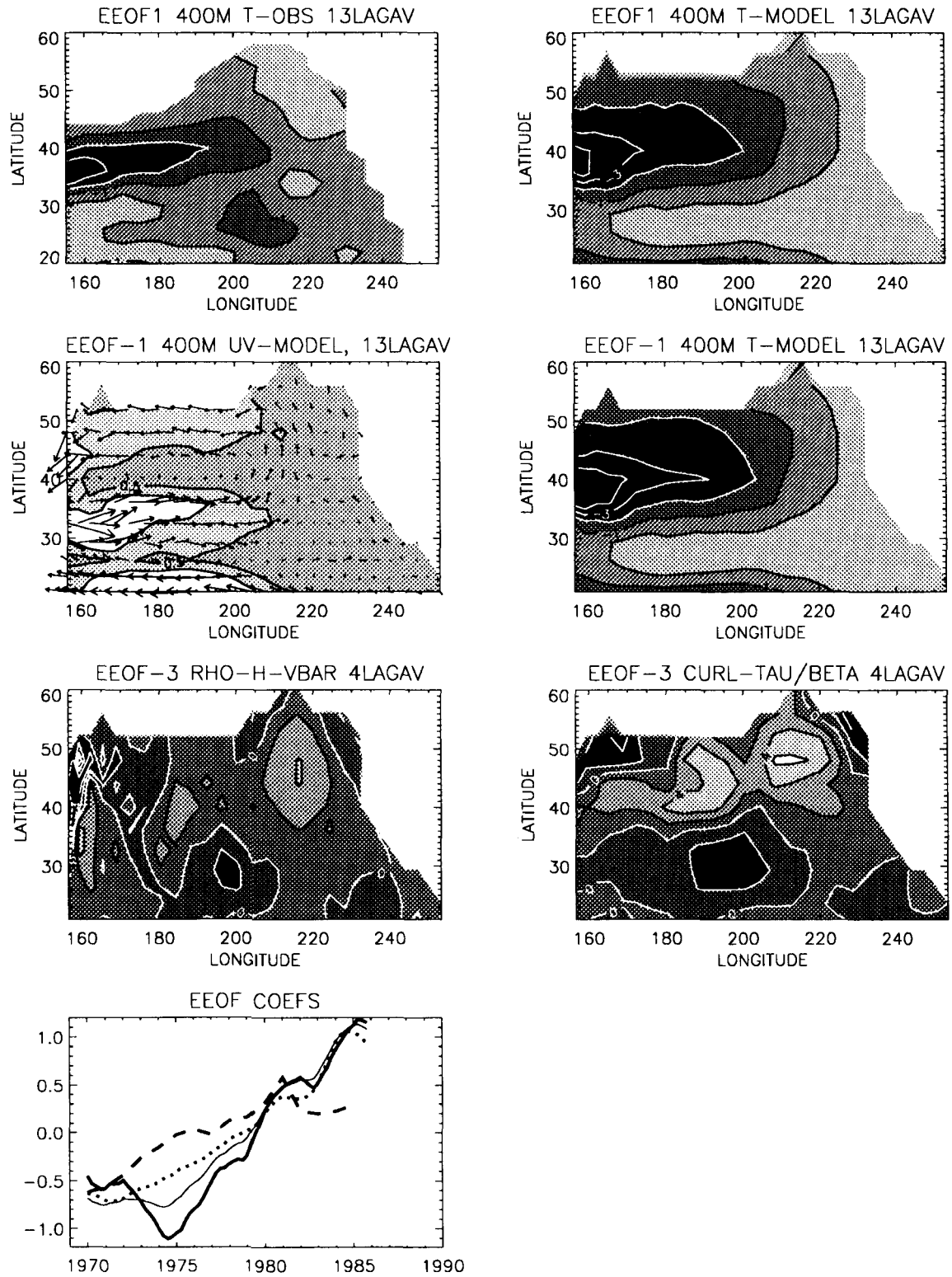
EEOF-3 CURL-TAU/BETA 4LAGAV

EEOF COEFS

Figure 3.   A synopsis of three separate combined extended EOF analyses. *Top*, Combined EEOF-1 of observed (*left*) and modeled (*right*) 400-m temperature, plotted as an average over all 13 lags. *Middle*, Same as top but for combined EEOF-1 of (*left*) model 400-m velocity and (*right*) model 400-m temperature. *Lower*, Combined EEOF-3 of north-south 0–1,500-m transport (scaled by density and depth) and wind stress curl over beta, plotted as an average over all 4 lags (0 to 3 years). *Bottom*, Corresponding principal components of top (*thin line*), middle (*dotted line*), and lower (*dashed line*) EEOFs, along with that of EEOF-1 of the observations alone (*thick line*), each scaled arbitrarily to fit on the same plot.

modes by the Gulf of California) propagating from the tropics.

Although high-resolution modeling studies have suggested that thermocline anomalies off California may be associated with wave radiation from coastally trapped waves of equatorial origin, unambiguous observational evidence has been lacking. In a recent study, however, Miller et al.[5] identified thermocline anomalies which propagated westward on ENSO time scales from western North America to near the dateline. Figure 4 shows maps of the observed fluctuations expressed as EEOFs. Westward-propagating 400-m temperature anomalies are clearly evident from 20°N up to 45°N, and they appear to reach as far west as the dateline, at which point they are either arrested or obscured by the ambient noise of the Kuroshio extension. Anomalies farther south in the analysis domain, near 20°N, propagate faster and farther westward, as anticipated. EEOF-3 leads EEOF-4 by approximately one year, as can be seen in the time series and in the map patterns, which are nearly identical when accounting for the one-year lag. The largest signals in the time series correspond to the mid-1980s and the mid-1970s and have a stochastic periodicity of 3–4 years.

Clearly, the signals in figure 4 are indicators of ENSO time-scale activity and suggest radiated baroclinic Rossby waves, which have been identified in aforementioned high-resolution numerical models in association with coastally trapped Kelvin-like waves of tropical origin. However, the thermocline waves identified here differ from the ones identified in those model studies in several respects. They have longer east-west wavelengths (roughly 3,000 km compared to 800–1,200 km) at 30°–45°N and therefore larger phase speeds (2.4 cm/s) than the thermocline anomalies associated with coastal variability of equatorial origin. Also their amplitude appears to increase away from the eastern boundary. Lastly, Miller et al.[6] show that they also occur in a low-resolution model in which, although it admits a poleward propagating Kelvin-like wave (e.g., O'Brien and Parham 1992), the numerical analogue Kelvin wave is seriously damped as it propagates northward and is trapped to one grid point in the offshore direction.

Miller et al.[7] explored the dynamics of the ENSO-scale thermocline anomalies of figure 4 by studying the model's version of the phenomenon. Figure 5 shows maps of three cases of the combined EEOFs (for brevity, only one lag of the analogue to EEOF-4 of figure 4 is shown; refer to figure 4 for information on phase propagation). The top panel of figure 5 features maps of one

phase (cf. figure 4, top right) of the combined EEOF of the observed and modeled thermocline anomalies, which show that the model captures the large-scale westward-propagating behavior and that the time series (bottom, thin line) is coherent with that of the observations alone (bottom; thick line is from EEOF-4 of figure 4). Figure 5 (middle panel, with time series at bottom, dotted line) also shows the combined EEOF of model 400-m temperature and velocity and reveals that the large-scale circulation anomalies associated with the thermocline perturbations are nearly geostrophically balanced. The velocity maps reveal large-scale coherent velocity perturbations that extend several thousand kilometers along the west coast of North America. Their magnitude along the eastern boundary exceeds 0.2 cm/s in the model, suggesting that observed anomalies would reach nearly 0.5 cm/s if we account for the weaker temperature signal found in the model vis-a-vis observations. As the velocity anomalies migrate westward away from the boundary they become more meridional and extend into/from the southern parts of the Alaska Gyre.

The bottom panel of figure 5 shows the combined EEOF of north-south integrated (0–1,500-m) velocity and curl τ scaled to allow for potential Sverdrup balance (time series at bottom, dashed line), as a preliminary investigation of the vorticity dynamics of the thermocline anomalies. Instead of nearly Sverdrup-balanced velocities as seen in the decadal mode, the model thermocline anomalies occur in phase with large-scale deepening and weakening of the Aleutian Low. This suggests that the midlatitude thermocline anomalies seen in the model (which mimic those observed, although the model anomalies are weaker) are significantly driven by mid-latitude forcing. It is unclear to what degree the midlatitude waves are forced by signals propagating along the eastern boundary, but, as previously mentioned, this model does not properly resolve this process, and models that do resolve the process yield shorter-wavelength thermocline anomalies.

Basinwide plots (not shown) of the full, unfiltered, seasonal thermocline anomalies for both model and observations reveal that the strongest signal is associated with the 1982–83 ENSO. One can follow the warm thermocline anomaly from the western North American coast across the basin until it encounters the western boundary (at low latitudes) and the Kuroshio region (in middle latitudes). The observed and modeled thermocline anomalies encounter the Kuroshio region in 1987–88, at which point they are no longer discernible because of the high variability there. It is interesting to note that these waves travel twice as fast as those identified by Jacobs et al. (1994; 1996[8]) in satellite-derived

[5]Miller, A. J., W. B. White, and D. R. Cayan. North Pacific thermocline variations on ENSO time scales. MS submitted to J. Phys. Oceanogr.
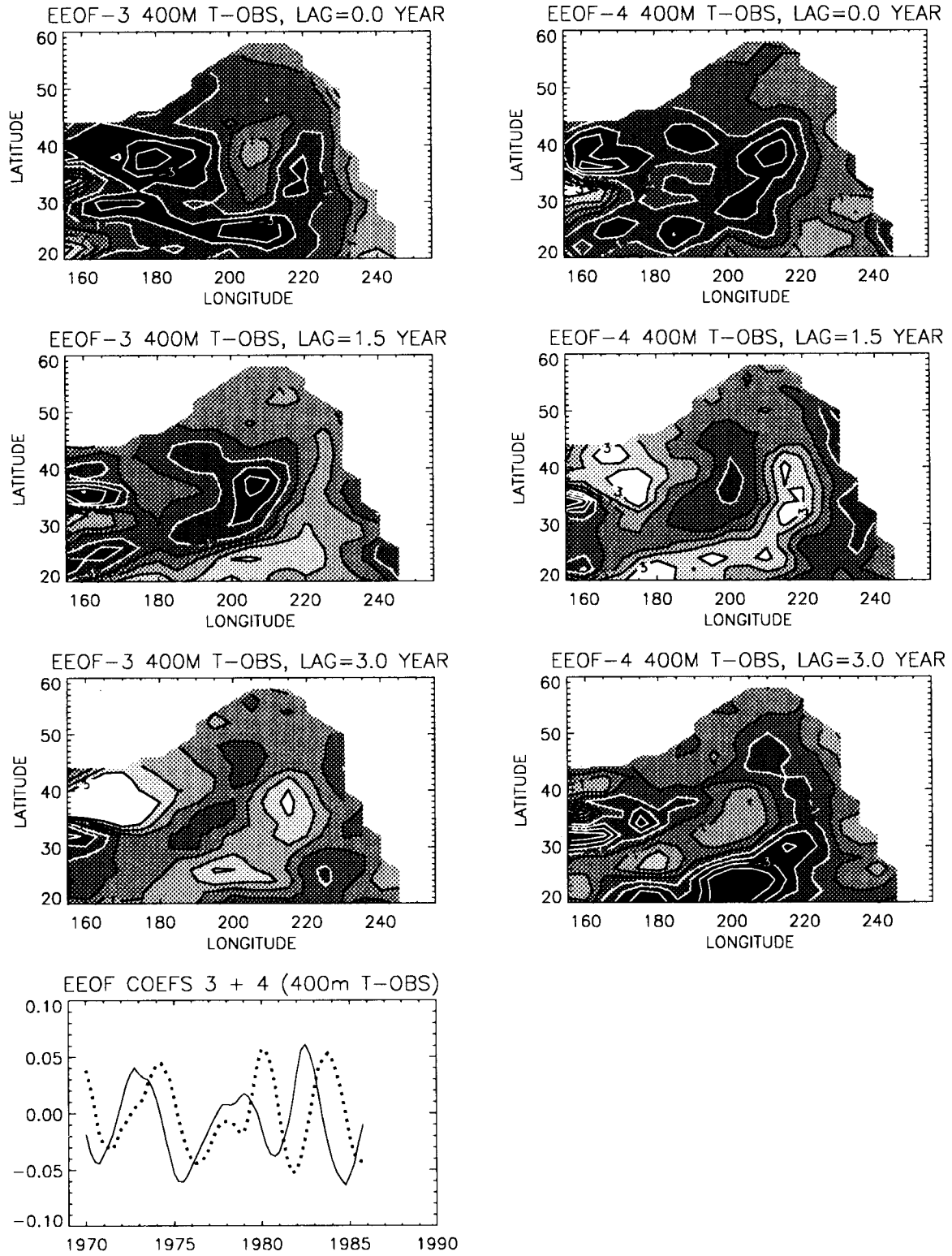[6]Ibid.
[7]Ibid.

[8]See footnote 4 on p. 72.

Figure 4. Third (*left*) and fourth (*right*) extended EOFs of the observed 400-m temperature alone for 3 of the 13 lags. *Top*, lag-0; *middle*, lag-1.5 yr; and *lower* lag-3 yr. *Bottom*, Corresponding principal components of third (*solid line*) and fourth (*dotted line*) EEOFs.
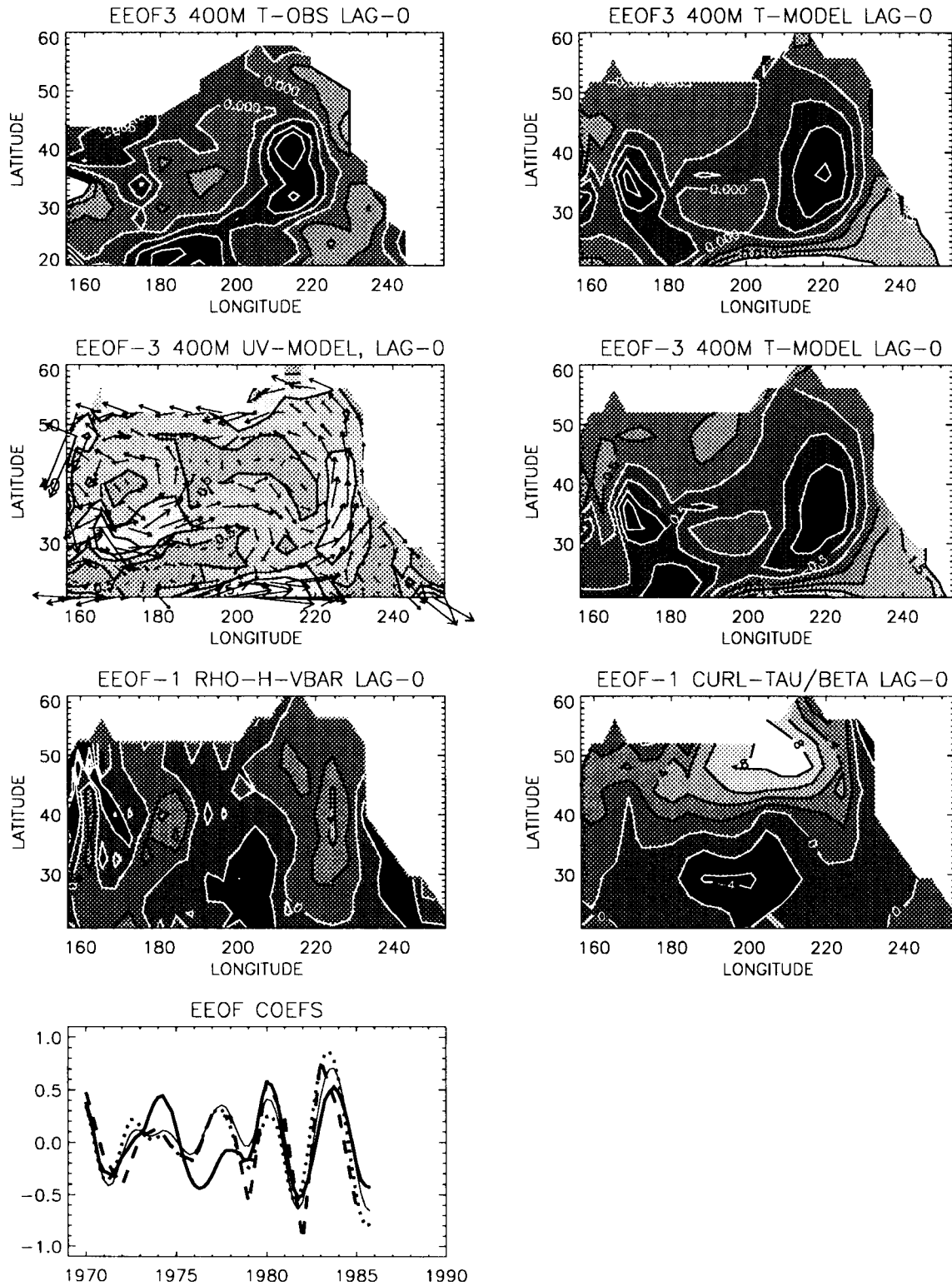
Figure 5.   As in figure 3, but for (top) EEOF-3, (middle) EEOF-3, and (lower) EEOF-1, each plotted only for lag-0 (refer to figure 3 EEOF-4 for phase propagation). Bottom, Corresponding principal components of top (thin line), middle (dotted line), and lower (dashed line) EEOFs, along with that of EEOF-4 (thick line) of the observations alone.
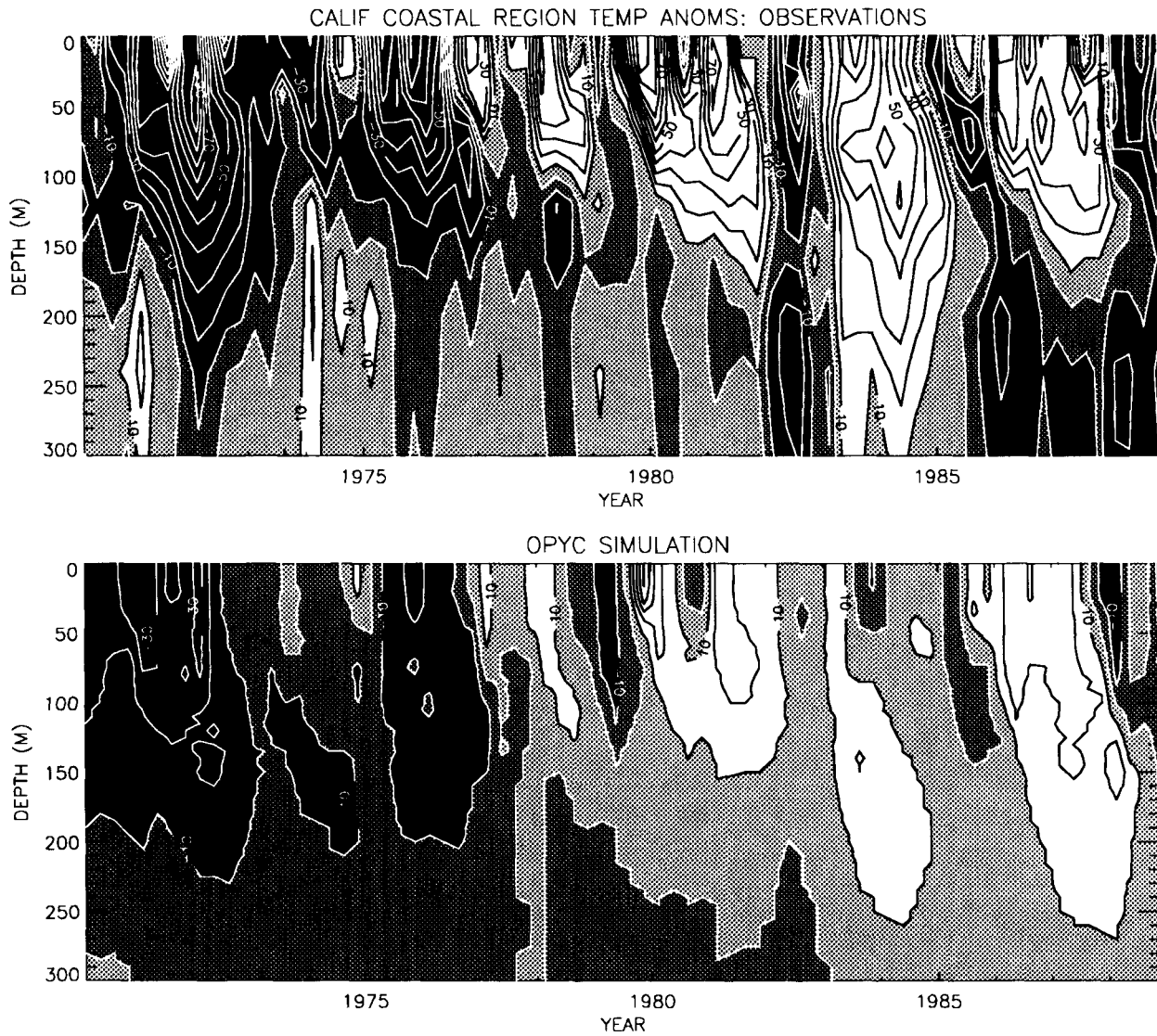
Figure 6.   Temperature anomalies averaged over the region 130°W–coast, 25°N–45°N from the surface to 300-m depth from 1970 to 1988 in the observations (top) and the model (bottom). Contour interval is 0.1°C (scaled by 100), with darker shades cooler and lighter shades warmer.

sea-level observations and high-resolution-model thermocline anomalies, which showed trans-Pacific transit times of nearly ten years of model thermocline anomalies and observed sea-level height anomalies. Chelton and Schlax (1996) also identified sea-level variations that travel twice as fast as their theoretical Rossby wave analogues. Basin-scale atmospheric forcing (e.g., figure 5) is a likely explanation for the increased phase speed.

DISCUSSION

A comparison of a relatively coarse-resolution model of the Pacific Ocean with observations of upper-ocean temperature reveals two dominant signals in the thermocline structure off the coast of California. The first signal is a thermocline deepening associated with a decadal-scale change in the gyre-scale North Pacific ther-

mocline. The second signal constitutes ENSO–time-scale waves propagating westward in the eastern North Pacific. The model suggests that the thermocline variations are both predominantly forced by wind stress curl.

Figure 6 gives a concise depiction of how these signals influence the large-scale thermocline off the California Coast (cf. Roemmich and McGowan 1995). The top panel shows the observations averaged over a region off western North America (130°W–coast, 25°N–45°N) as a function of depth and time, with the bottom showing the model version of reality. Although the decadal thermocline change has its strongest component in the northwestern part of the North Pacific, it is associated with a deepening of the thermocline (warmer ocean above 200 m) along the eastern boundary as well.
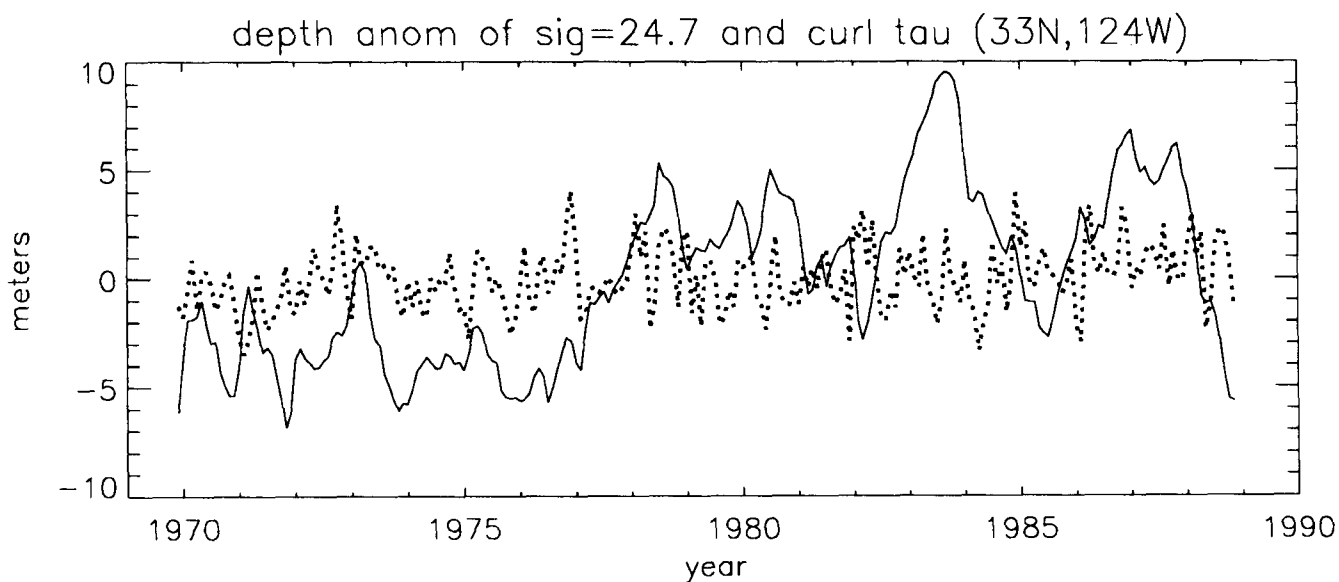
Figure 7. Depth anomalies (*solid line*) of the model isopycnal layer (sigma 24.7) at a grid point off the California coast. Positive anomalies indicate a deeper thermocline at mean level of roughly 180 m. Local wind stress curl anomalies (*dotted line*) at the same point.

Figure 7 shows depth anomalies of a model isopycnal layer (24.7 sigma layer) with a mean depth of roughly 180 m. One can see that the model thermocline deepens by 5–10 meters during the mid-1970s, although in the observations the change is larger and at a shallower depth than in the model (as can be seen in figure 6). Also shown in figure 7 is the local wind stress curl, which reveals no obvious correlation to the local thermocline anomalies; the basin-scale effect of the wind stress curl is instead the key factor.

Besides the decadal change, the ENSO time-scale thermocline fluctuations are evident in figures 6 and 7 as well. These interannual events are dynamically distinct from the decadal change, last for roughly one year, and are associated with temperature anomalies with local maxima at 50–100-m depth in the observations (cf. Norton and McLain 1994) and somewhat deeper maxima in the model (50–150 m).

Several interesting future studies need to be accomplished. There is substantial interest in longer interdecadal simulations with higher resolution than the hindcast discussed here. Such a model could be used for relating present climate variations to those of past centuries and for diagnosing the physical variables that influenced past biological regimes. Further research using idealized interannual forcing is also required to isolate the components of midlatitude ocean response driven by the midlatitude atmosphere versus the eastern boundary-wave propagation mechanism. Particular emphasis in this case should be placed on representing basin-scale atmospheric forcing, allowing interaction with basin-scale circulation, and understanding how thermocline variations affect SST. The most formidable task involves developing models that properly represent the large-scale eddy and small-scale filament formation processes which dominate the synoptic variations of the CCS. Nesting extremely high-resolution models in lower-resolution basin-scale models could aid in understanding how the large-scale flows and temperature variations influence instability processes, as well as their joint effect on associated biological systems.

ACKNOWLEDGMENTS

LITERATURE CITED

Allen, J. S., L. J. Walstad, and P. A. Newberger. 1991. Dynamics of the Coastal Transition Zone Jet. 2. Nonlinear finite amplitude behavior. J. Geophys. Res. 96:14,995–15,016.

Auad, G., A. Pares-Sierra, and G. K. Vallis. 1991. Circulation and energetics of a model of the California Current System. J. Phys. Oceanogr. 21:1534–1552.

Batteen, M. L., R. L. Haney, T. A. Tielking, and P. G. Renaud. 1989. A numerical study of wind forcing of eddies and jets in the California Current System. J. Mar. Res. 47:493–523.

Cayan, D. R. 1992. Latent and sensible heat flux anomalies over the northern oceans: driving the sea surface temperature. J. Phys. Oceanogr. 22: 859–881.

Chelton, D. B., and M. G. Schlax. 1996. Global observations of oceanic Rossby waves. Science 272:234–238.

Deser, C., M. A. Alexander, and M. S. Timlin. In press. Upper ocean thermal variations in the North Pacific during 1970–1991. J. Clim.

Douglas, A. V., D. R. Cayan, and J. Namias. 1982. Large-scale changes in North Pacific and North American weather patterns in recent decades. Monthly Weather Rev. 110:1851–1862.

Ebbesmeyer, C. C., D. R. Cayan, D. R. McLain, F. H. Nichols, D. H. Peterson, and K. T. Redmond. 1991. 1976 step in the Pacific climate: forty environmental changes between 1968–75 and 1977–1984. *In* Proc. 7th Ann. Pacific Climate Workshop, Calif. Dep. Water Resources, Interagency Ecol. Stud. Prog. Rep. 26.

Graham, N. E. 1994. Decadal scale variability in the 1970's and 1980's: observations and model results. Clim. Dynamics 10:135–162.

Haidvogel, D. B., A. Beckmann, and K. S. Hedstrom. 1991. Dynamical simulations of filament formation and evolution in the Coastal Transition Zone. J. Geophys. Res. 96:15,017–15,040.

Hurlburt, H. E., A. J. Wallcraft, Z. Sirkes, and E. J. Metzger. 1992. Modeling of the global and Pacific Oceans: on the path to eddy-resolving ocean prediction. Oceanography 5:9–18.

Jacobs, G. A., H. E. Hurlburt, J. C. Kindle, E. J. Metzger, J. L. Mitchell, W. J. Teague, and A. J. Wallcraft. 1994. Decade-scale trans-Pacific propagation and warming effects of an El Niño anomaly. Nature 370:360–363.

Johnson, M. A., and J. J. O'Brien. 1990. The northeast Pacific Ocean response to the 1982–83 El Niño. J. Geophys. Res. 95:7155–7166.

Lagerloef, G. S. E. 1995. Interdecadal variations in the Alaska Gyre. J. Phys. Oceanogr. 25:2242–2258.

McCreary, J. P., Y. Fukamachi, and P. Lu. 1992. A nonlinear mechanism for maintaining coastally trapped eastern boundary currents. J. Geophys. Res. 97:5677–5692.

Meyers, S. D., M. A. Johnson, M. Liu, J. J. O'Brien, and J. L. Spiesberger. In press. Interdecadal variability in a numerical model of the northeast Pacific Ocean. 1970–89. J. Phys. Oceanogr.

Miller, A. J., D. R. Cayan, T. P. Barnett, N. E. Graham, and J. M. Oberhuber. 1994a. Interdecadal variability of the Pacific Ocean: model response to observed heat flux and wind stress anomalies. Clim. Dynamics 9:287–302.

———. 1994b. The 1976–77 climate shift of the Pacific Ocean. Oceanography 7:21–26.

Moisan, J. R., and E. E. Hofmann. In press. Modeling nutrient and plankton processes in the California Coastal Transition Zone. 1. A time and depth dependent model and 3. Lagrangian drifters. J. Geophys. Res.

Moisan, J. R., E. E. Hofmann, and D. B. Haidvogel. In press. Modeling nutrient and plankton processes in the California Coastal Transition Zone. 2. A three-dimensional physical-bio-optical model. J. Geophys. Res.

Norton, J. G., and D. R. McLain. 1994. Diagnostic patterns of seasonal and interannual temperature variation off the west coast of the United States: local and remote large-scale atmospheric forcing. J. Geophys. Res. 99: 16,019–16,030.

Oberhuber, J. M. 1993. Simulation of the Atlantic circulation with a coupled sea ice–mixed layer–isopycnal general circulation model. Part I: Model description. J. Phys. Oceanogr. 22:808–829.

O'Brien, J. J., and F. Parham. 1992. Equatorial Kelvin waves do not vanish. Monthly Weather Rev. 120:1764–1767.

Pares-Sierra, A., and J. J. O'Brien. 1989. The seasonal and interannual variability of the California Current System. J. Geophys. Res. 94:3159–3180.

Philander, S. G. H., and J.-H. Yoon. 1982. Eastern boundary currents and coastal upwelling. J. Phys. Oceanogr. 12:862–879.

Ramp, S. R., J. L. McClean, C. A. Collins, A. J. Semtner, and K. A. S. Hays. In press. Observations and modeling of the 1991–1992 El Niño signal off central California. J. Geophys. Res.

Rienecker, M. M., C. N. K. Mooers, and A. R. Robinson. 1987. Dynamical interpolation and forecast of the evolution of mesoscale features off northern California. J. Phys. Oceanogr. 17:1189–1213.

Robinson, A. R., J. A. Carton, C. N. K. Mooers, L. J. Walstad, E. F. Carter, M. M. Rienecker, J. A. Smith, and W. G. Leslie. 1984. A real-time dynamical forecast of ocean synoptic/mesoscale eddies. Nature 309:781–783.

Roemmich, D., and J. McGowan. 1995. Climatic warming and the decline of zooplankton in the California Current. Science 267:1324–1326.

Sekine, Y. 1991. Anomalous southward intrusion of the Oyashio east of Japan. I. Influence of the interannual and seasonal variations in the wind stress over the North Pacific. J. Geophys. Res. 93:2247–2255.

Shriver, J. F., M. A. Johnson, and J. J. O'Brien. 1991. Analysis of remotely forced oceanic Rossby waves off California. J. Geophys. Res. 96:749–757.

Smith, R. D., J. K. Dukowicz, and R. C. Malone. 1992. Parallel ocean general circulation modeling. Physica D 60:38–61.

Tabata, S. 1991. Annual and interannual variability of baroclinic transports across Line P in the northeast Pacific Ocean. Deep-Sea Res. 38(S1): S221–S245.

Trenberth, K. E. 1990. Recent observed interdecadal climate changes in the Northern Hemisphere. Bull. Am. Meteorol. Soc. 71:988–993.

Trenberth, K. E., and J. W. Hurrell. 1994. Decadal atmosphere-ocean variations in the Pacific. Clim. Dynamics 9:303–319.

White, W. B. 1995. Design of a global observing system for gyre-scale upper ocean temperature variability. Prog. Oceanogr. 36:169–217.